



Discover Generics

Cost-Effective CT & MRI Contrast Agents

 **FRESENIUS
KABI**

[WATCH VIDEO](#)

AJNR

Study of Movement Disorders and Brain Iron by MR

J. Neal Rutledge, Sadek K. Hilal, A. John Silver, Richard Defendini and Stanley Fahn

AJNR Am J Neuroradiol 1987, 8 (3) 397-411
<http://www.ajnr.org/content/8/3/397>

This information is current as of June 22, 2025.

Study of Movement Disorders and Brain Iron by MR

J. Neal Rutledge^{1,2}
 Sadek K. Hilal¹
 A. John Silver¹
 Richard Defendini³
 Stanley Fahn⁴

Heavily T2-weighted high-field MR images provide a unique opportunity for the evaluation of the extrapyramidal motor system. The images are affected by the presence of small amounts of naturally occurring paramagnetic substances—principally iron—that delineate the neostriatum (caudate and putamen), globus pallidus, red nucleus, substantia nigra, and dentate nucleus, primarily by a decrease in signal secondary to the T2* effect. Movement disorders are associated with either increased or decreased signal or both in these structures, depending on the pathologic process. In the initial evaluation of 113 patients with a variety of movement disorders, good correlation of imaging abnormalities can be made with a simplified schema of the extrapyramidal pathways and a system of classification of abnormal movements, parkinsonism/tremor, dystonia, chorea, myoclonus, and hemiballismus. Parkinsonisms are characterized by abnormalities of the cortico-ponto-cerebello-dentato-rubro-thalamo-cortico-spinal tract or the nigrostriatal tract. Dystonias are characterized by abnormalities of the neostriatum predominantly affecting the putamen. Chorea are also characterized by abnormalities of the neostriatum but predominantly affecting the caudate nucleus. Hemiballismus is characterized by lesions affecting the subthalamic nucleus or associated pathway.

Iron

Interest in movement disorders is heightened by the recent ability to map the distribution of macromolecular complexes of Fe(III) in the brain with heavily T2-weighted images. This is accomplished through contrast created by the T2* effect, a local inhomogeneity in the magnetic field that dephases spin and results in loss of signal [1]. This effect is different from the paramagnetic effect of smaller soluble contrast agents, such as gadolinium, and corresponds roughly with the ferric iron distribution demonstrated by Perls' Prussian blue reaction (Fig. 1) [2].

The signal loss observed varies according to the concentration of the macromolecular complexes and the square of the field strength. Normally a statistically characteristic distribution of iron exists that varies with age: none is present at birth; then a rapid accumulation of iron occurs with the majority being present between the ages of 8 and 25 years. After this, a gradual accumulation occurs with prominence seen in the globus pallidus, putamen, and substantia nigra in old age [3–5].

It is a unique characteristic of the extrapyramidal system that its nuclei contain high concentrations of iron. Especially rich are the substantia nigra and globus pallidus. Lesser amounts of iron are found in the red nucleus, dentate nucleus, nigrostriatal tract, putamen, caudate nucleus, and the fifth layer of cortical gray matter [6]. The reasons for increased concentration of iron in nuclei related to movement are unknown; these reasons are reviewed in our discussion.

Other trace metals found in the brain in significant amounts include copper, magnesium, and zinc [3, 4]. In the normal state they appear to contribute little to MR imaging. But in pathologic states, for example, Wilson's disease with increased copper concentrations, their effect becomes apparent and applicable to the study of the extrapyramidal system.

This article appears in the May/June 1987 issue of *AJNR* and the August 1987 issue of *AJR*.

Received July 10, 1986; accepted after revision November 20, 1986.

Presented at the annual meeting of the American Society of Neuroradiology, San Diego, January 1986.

This work was supported in part by National Institutes of Health grant CA 28881 and by Philips Medical Systems, Inc.

¹ Department of Radiology, Division of Neuro-radiology, Columbia-Presbyterian Medical Center, New York, NY 10032.

² Present address: 10 Medical Arts Square, Austin, TX 78705. Address reprint requests to J. N. Rutledge.

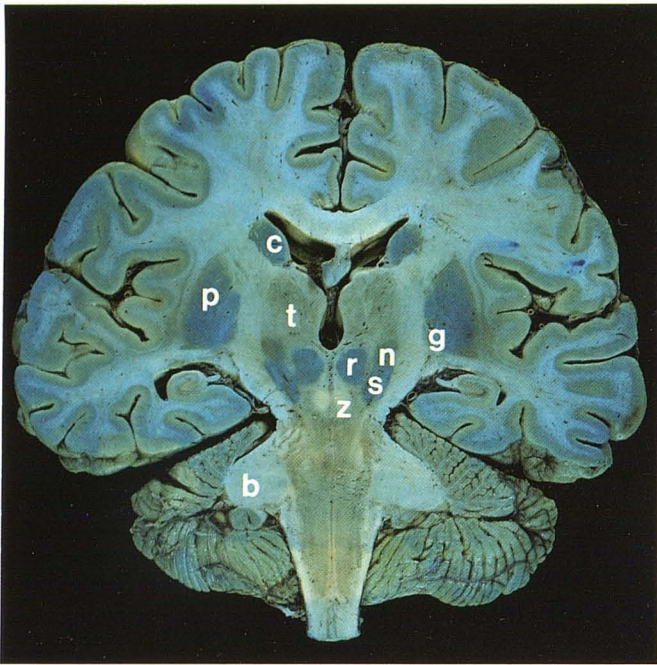
³ Department of Pathology, Division of Neuro-pathology, Columbia-Presbyterian Medical Center, New York, NY 10032.

⁴ Department of Neurology, Division of Movement Disorders, Columbia-Presbyterian Medical Center, New York, NY 10032.

AJNR 8:397–411, May/June 1987

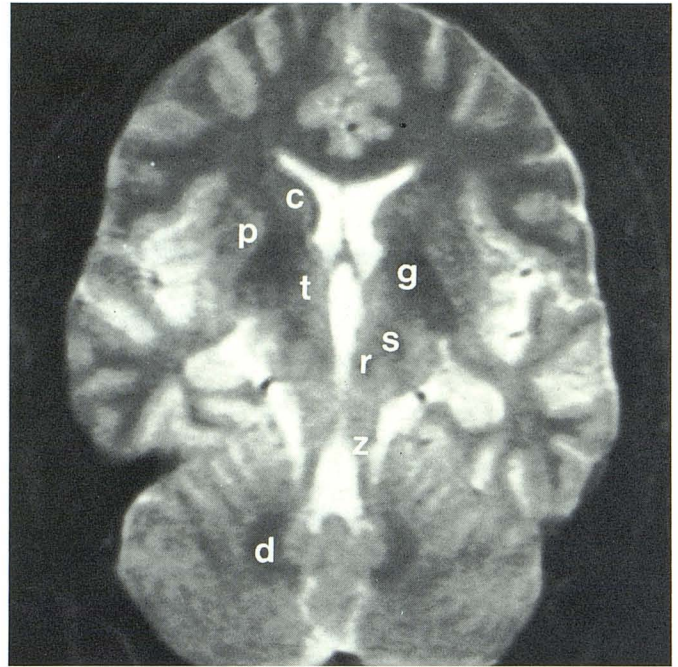
0195–6108/87/0803–0397

© American Society of Neuroradiology



A

Fig. 1.—Semicoronal sections of normal brain. A, Perls' stain in 47-year-old shows most extrapyramidal nuclei and tracts.



B

B, Heavily T2-weighted MR image in 30-year-old shows decreased signal in corresponding extrapyramidal nuclei. c = caudate nucleus; p = putamen; t = thalamus; g = globus pallidus; n = subthalamic nucleus; r = red nucleus; z = brachium conjunctivum; b = brachium pontis; s = substantia nigra; d = dentate nucleus.

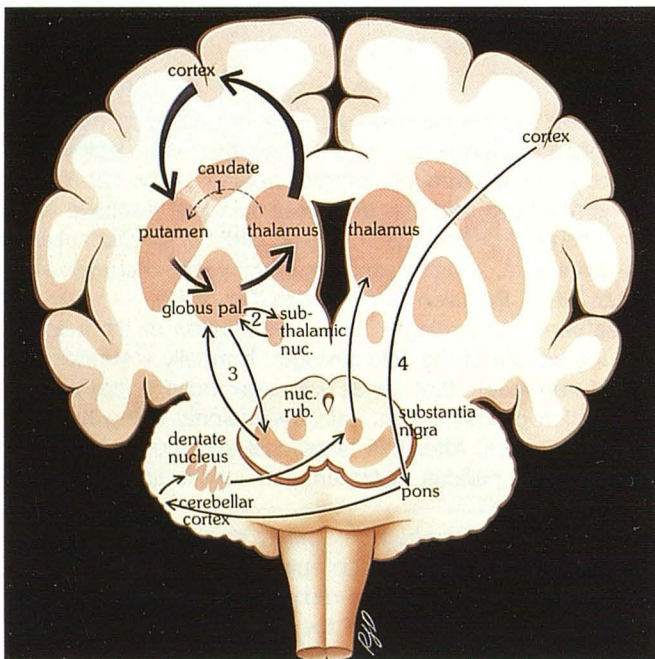


Fig. 2.—Simplified extrapyramidal pathway shows circuits frequently involved in movement disorders: dystonias and choreas (loop 1), hemiballismus (loop 2), and parkinsonisms (loops 3 and 4).

Movement Disorders

Classically, movement has been found to be mediated by multiple neural pathways that can be divided into pyramidal, extrapyramidal, and cerebellar systems. This classification, however, belies the fact that multiple coordinated interaction between these artificial divisions is required for purposeful movement. In the radiologic conceptualization of movement disorders, a simplified model of the involved anatomic pathways can be useful. The extrapyramidal system can then be thought of as a major circuit and several minor circuits that modify the control of movement. Damage to these circuits causes involuntary movement and other nonparalytic disorders by release of inhibition, dyscoordination, or loss of modulation on the pyramidal tract.

The major extrapyramidal motor circuit is a loop consisting of projections from the cortex to the neostriatum (caudate and putamen nuclei), globus pallidus, thalamic nuclei, and finally returning to the cortex (see loop 1 in Fig. 2). Damage to this circuit is manifest by signal changes on MR and results in a clinically manifest spectrum of abnormal movements ranging from dystonia to chorea. Accessory or minor extrapyramidal motor circuits are formed between the subthalamic nucleus and globus pallidus (see loop 2 in Fig. 2); the lenticular nuclei (caudate, putamen, and globus pallidus) and substantia nigra (loop 3); and a complex loop originating in the cortex, passing through the pons, brachium pontis, and cerebellum

TABLE 1: Definitions of Terms Descriptive of Movement Disorders

Term	Definition
Tremor	Involuntary, rhythmic, oscillatory movements of opposing muscles
Myoclonus	Abrupt, shocklike contraction of a single or group of muscles
Hemiballismus	Sudden, violent, swinging movements of arm and/or leg
Dystonia	Usually slow, sustained, continual, repetitive, and twisting contractions that can result in postural abnormality
Athetosis	Slow, sinuous, writhing, purposeless movements flowing into one another
Chorea	Rapid, arrhythmic, nonrepetitive, nontwisting, flowing movements affecting proximal and distal muscles

and returning to the thalamus via the brachium conjunctivum and red nucleus (cortico-ponto-cerebello-dentato-rubro-thalamo-cortico-spinal tract, loop 4). Hemiballismus is caused by damage to loop 2. Parkinsonisms result from damage to loops 3 and/or 4 [7, 8].

Understanding the extrapyramidal system is made more difficult by the classification and description of the resulting abnormal movements. The definitions set out in Table 1 were used in this study [9]. Patients were then grouped according to these definitions, and their images correlated for specific changes. Athetosis was not assessed separately because of the lack of characteristic pathologic changes and difficulty distinguishing it clinically from a chorea or a dystonia.

Subjects and Methods

To analyze the phenomenon of decreased signal delineating the extrapyramidal system, eight pathologic specimens 8–72 years old were stained for iron and compared with normal heavily T2-weighted images. One hundred thirteen patients with a variety of movement disorders were then imaged and assessed for differences in signal patterns.

The pathologic specimens were prepared for iron staining by preserving them in formalin for 5 days, instead of the conventional 4 weeks, to minimize any leaching of the iron. They were then sectioned and stained in a two-step process: 15 min in 2.5% potassium ferrocyanide only and 15 min in 1% hydrochloric acid [10]. This results in Perls' Prussian blue reaction, with maximum color-contrasting areas containing ferric iron (Fig. 3). Prolonging the staining process tends to reduce the intensity differences.

The MR images were obtained using a 1.5-T prototype system (Columbia-Philips). A spin-echo pulse sequence was used with an echo time (TE) of 70–120 msec and a repetition time (TR) of 4300 msec along with an acquisition matrix of 512 × 768 or 256 × 768 to produce contiguous 5-mm slices, primarily in the axial plane.

Between October 1984 and September 1985 113 consecutive patients with a variety of movement disorders were studied. The patients were 3 months to 78 years old. IV sedation was required in most cases. The images were grouped according to the type of abnormal movement and assessed for any signal changes. In the

subgroup of parkinsonisms 30 age-matched controls were used to help assess subtle changes and their significance. The images were then grouped according to clinical diagnosis to assess any further characteristics.

Results

Iron Staining

Excellent demonstration of the nuclei containing ferric iron is obtained by the methods outlined by Gans [10]. Extrapyramidal nuclei stain a deep blue color in a dynamic process corresponding to their concentrations of iron, as documented by Harrison et al. [3] (Table 2).

Other staining occurs near the gray-white-matter border in the deep cortical gray layers and is easily mistaken for white-matter U fibers (Fig. 3F). Also the frontal white matter is usually noted to stain more deeply than the occipital white matter.

Areas with lack of staining are also present. The internal capsule, corpus callosum, and anterior and posterior commissures show little staining grossly. Closer inspection of the internal capsule demonstrates fine, intensely staining tracts traversing it (Fig. 4).

The optic system is also dramatically devoid of staining. The optic tracts, lateral geniculate body, and optic radiations can all be seen to stain less than adjacent white matter.

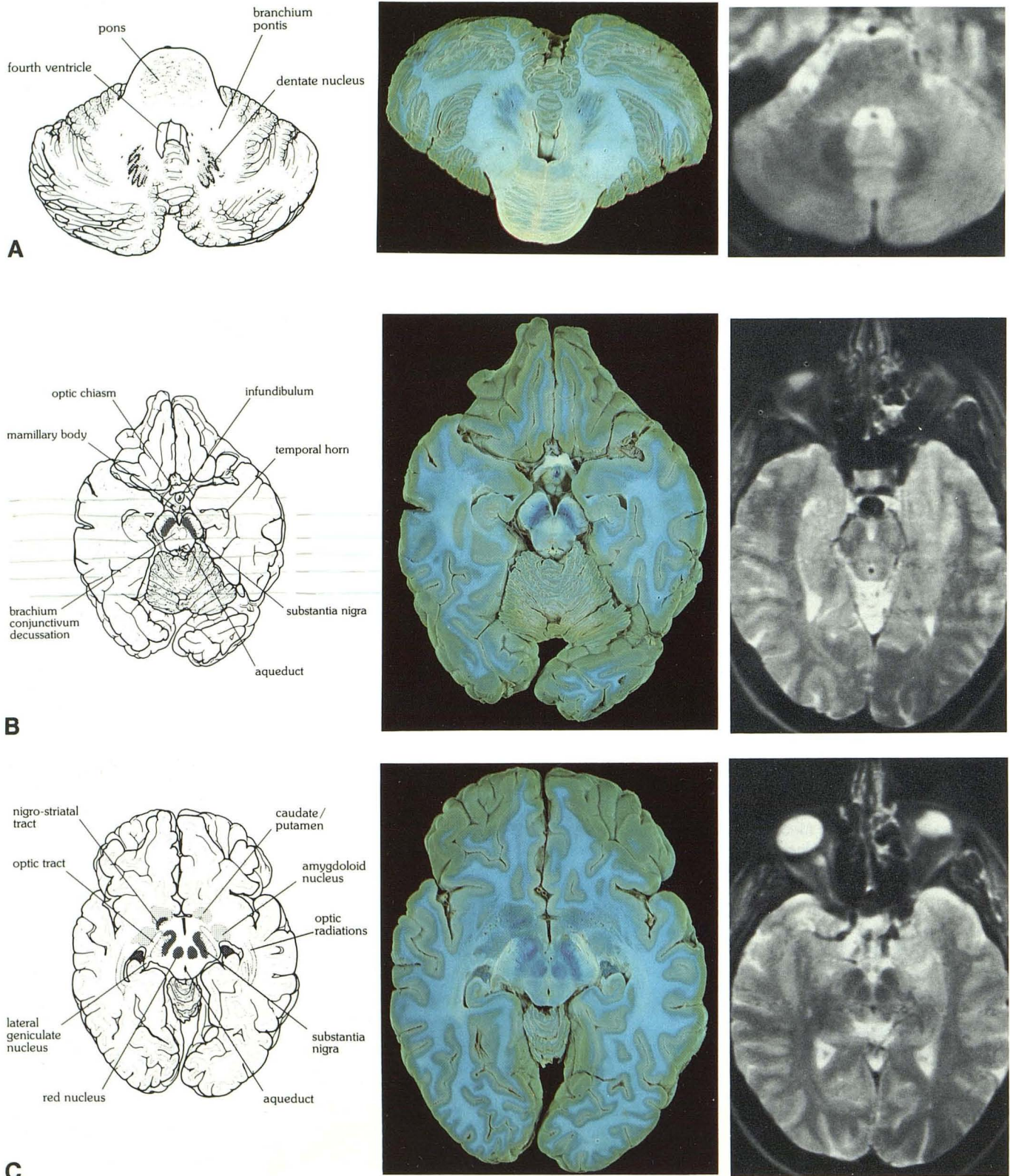
An important observation is the intensity with which caudate and putamen stain. Even considering the naturally darker color of the neostriatum, the amount of ferric iron staining present is intense. This is significant when comparison is made with the MR images.

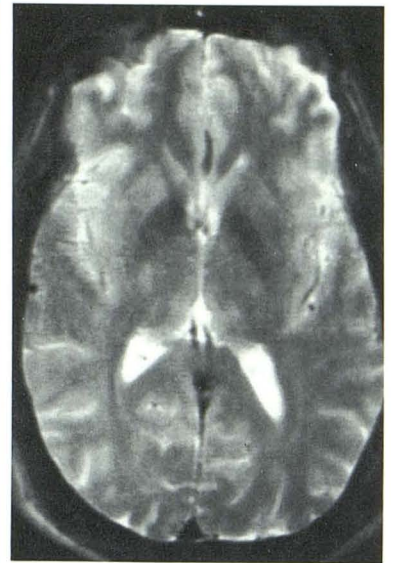
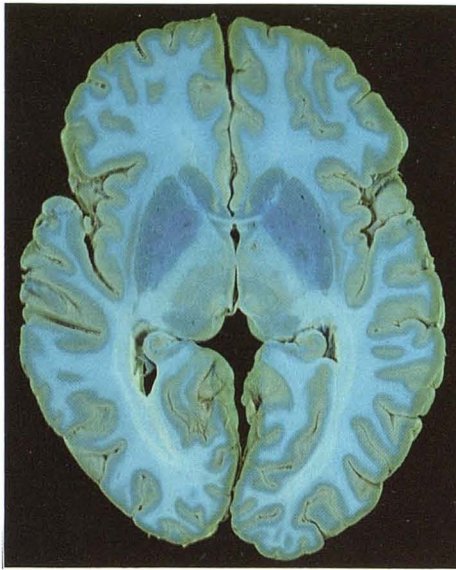
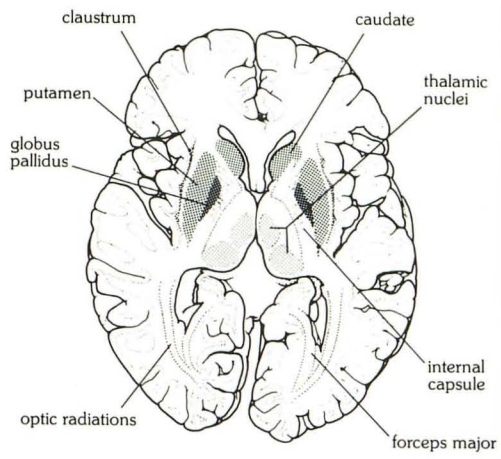
MR Images

Comparison of the heavily T2-weighted images and Perls' stain shows a close but imperfect relationship between the signal void on MR and the intensity of the stain. The low signal intensity seen in the substantia nigra, red nucleus, dentate nucleus, globus pallidus, deep cortical layers, and some white-matter areas correlates perfectly with the stained specimens (Figs. 3 and 4). Areas like the optic system (optic tract, radiations, and lateral geniculated body) also correlate closely. This includes an area of high signal commonly seen at the posterior end of the putamen, the pars retrolenticularis of the optic tract. This has been attributed to the internal capsule [11] (Fig. 3C).

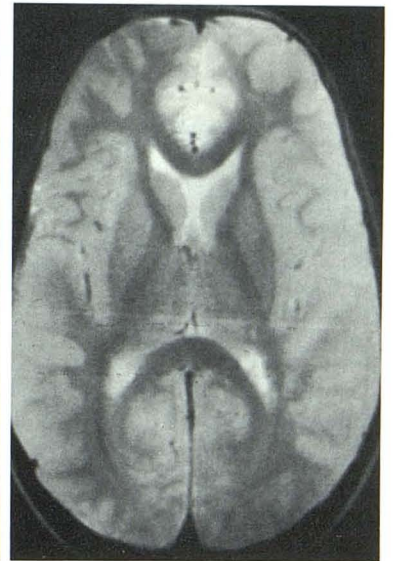
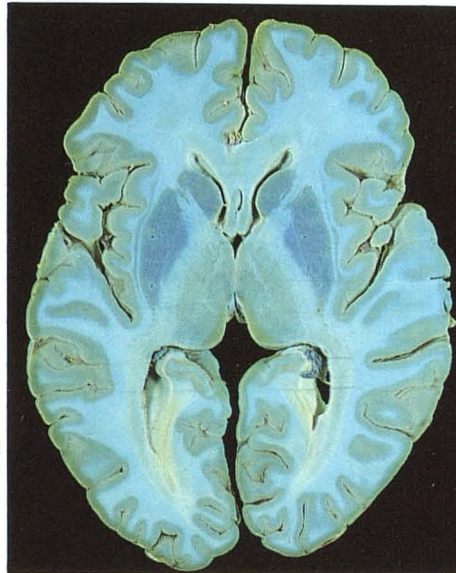
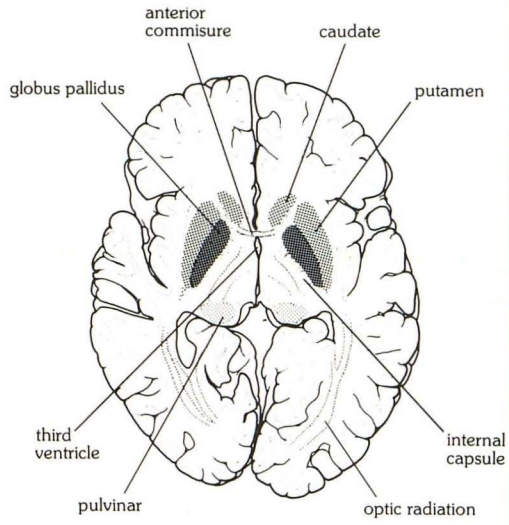
In contrast to previous observers, we did not find that MR signal correlation between Perls' stain and the signal void exists everywhere. The putamen and caudate show relatively little loss in signal when compared with the loss expected by the iron concentration or Perls' stain. Also the internal capsule, commissures, and corpus callosum show a much larger decrease in signal than Perls' stain predicts (Fig. 4A). This lack of correlation will be discussed.

Fig. 3.—Axial diagrams (left) corresponding to Perls' stain (middle) and heavily T2-weighted MR images (right) in normal 25-year-old document correlation between regions of ferric staining and signal loss.

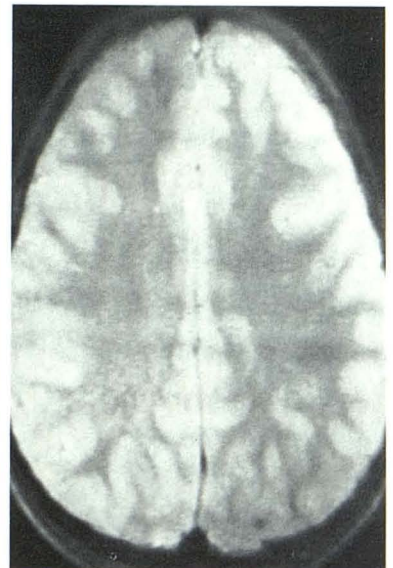
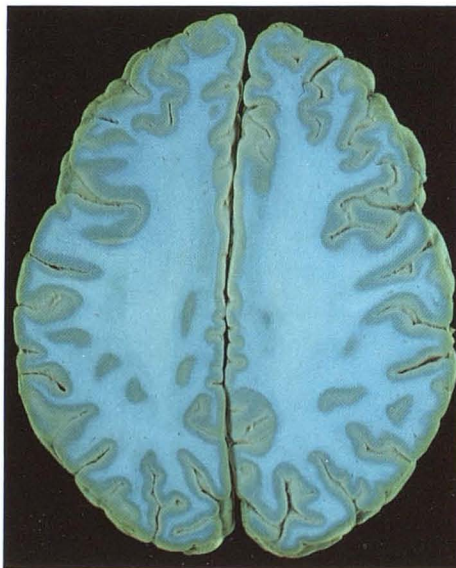
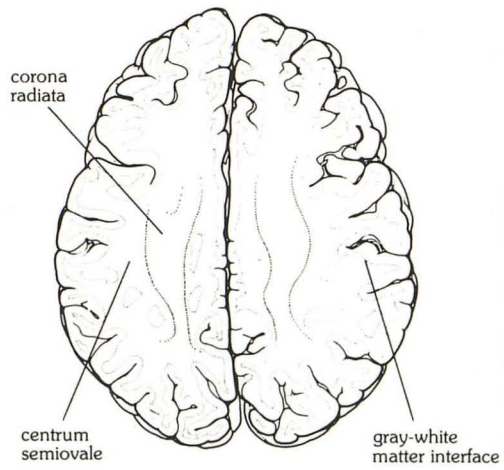




D



E



F

Parkinsonisms and Myoclonus

Thirty-five patients with parkinsonism/tremors were studied (Table 3). All patients had been treated pharmacologically at least 3 years before being imaged. These were compared with 30 age-matched controls who had no symptoms of parkinsonism or other abnormalities.

The most common abnormality identified was a restoration of signal in the area of void normally observed in the dorsal lateral aspect of the substantia nigra seen at the superior collicular level of the midbrain. By restoration we mean that the decreased signal seen in normal patients was changed to a signal level similar to that of brain parenchyma without iron. In patients with parkinsonism, 75% showed restoration of signal, while only 53% of age-matched patients (without symptoms) showed this change (Figs. 3C and 5). The odds ratio for this finding is 2.63 with a 90% confidence interval (0.76–9.10). The sample size is too small for a significant chi square.

Comparison of degrees of general atrophy demonstrated increased atrophy in 86% of patients with parkinsonism vs

56% in age-matched controls. Focal atrophy was found to be an excellent marker of secondary parkinsonism and the heterogeneous system degenerations, being present at least to some degree in 73%. This focal atrophy was not present in the control group. A loss of signal seen by other examiners [12, 13] in the dorsal lateral aspect of the putamen was seen in 20 (67%) of our 30 normal controls and was associated with increasing age (Fig. 6). We found a similar amount of decreased signal in 25 (71%) of the 35 patients with parkinsonism.

Greater correlation occurred after separating these patients into subgroups corresponding to their clinical diagnosis. Of the 12 patients with primary parkinsonism (Parkinson's disease), no additional changes were noted, but among second-

TABLE 2: Elemental Concentrations of Iron in Brain Tissue

Region	mg Fe/100 g Tissue
Globus pallidus	21.3
Red nucleus	19.5
Substantia nigra	18.5
Putamen	13.2
Dentate nucleus	10.4
Caudate nucleus	9.3
Thalamus	4.8
Cerebellar cortex	3.4
Motor cortex	5.0
Prefrontal cortex	3.0
Frontal white matter	4.2
Liver	13.4

TABLE 3: MR Findings in Parkinsonian Syndromes

Group: Finding	No.
Parkinsonism (<i>n</i> = 35):	
Striatonigral tract abnormality (restoration of signal in substantia nigra)	25
Cortico-ponto-cerebello-dentate tract abnormality (focal atrophy or increased signal)	23
Generalized atrophy	30
Decreased signal in dorsolateral putamen	25
Normal age-matched controls (<i>n</i> = 30):	
Decreased signal in dorsolateral putamen	20
Restoration of signal in substantia nigra	16
Parkinson's disease (<i>n</i> = 12):	
Restoration of signal in substantia nigra	9
Secondary parkinsonism—infarct (<i>n</i> = 4):	
Striatonigral tract abnormality	3
Cortico-ponto-cerebello-dentate tract abnormality	4
Heterogeneous system degenerations (<i>n</i> = 19):	
Striatonigral tract abnormality	13
Cortico-ponto-cerebello-dentate tract abnormality	19

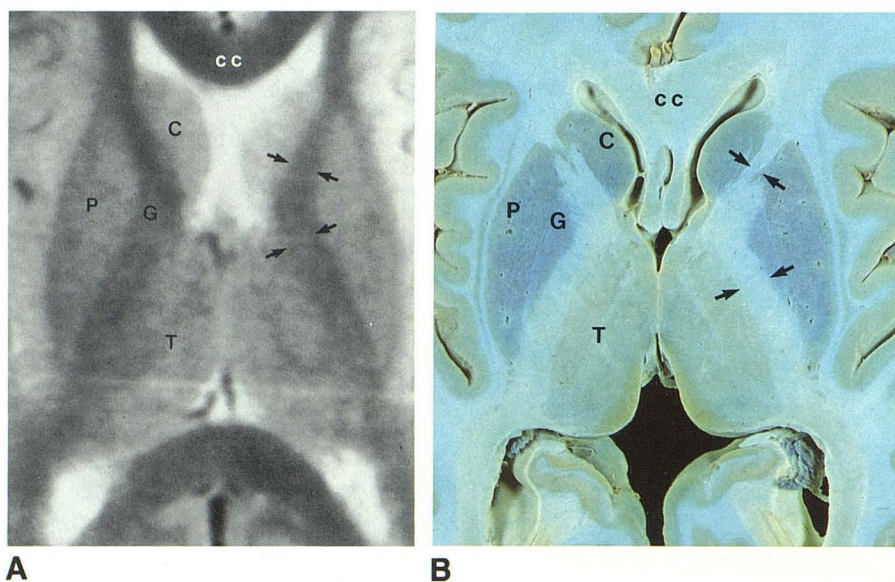
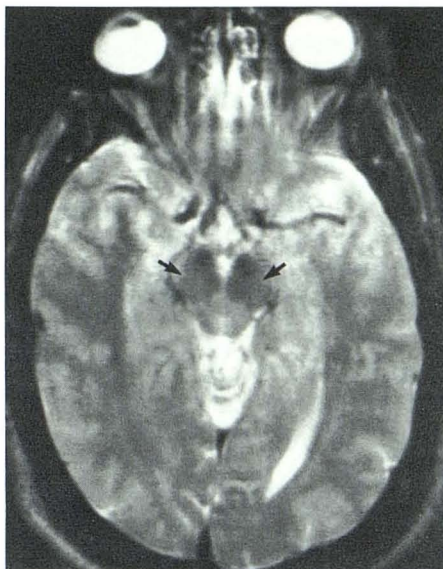


Fig. 4.—Magnified axial MR image (A) and Perls' stain (B) show areas of greatest disparity between ferric staining and signal loss. Caudate nucleus (C) and putamen (P) are stained without signal loss. Internal capsule (arrows) and corpus callosum (cc) show little staining and moderate signal loss. G = globus pallidus; T = thalamus; or = optic radiations.

Fig. 5.—Axial, 1.5-T SE 4300/80 image of Parkinson's disease shows restoration of signal in dorsal lateral substantia nigra (arrows).



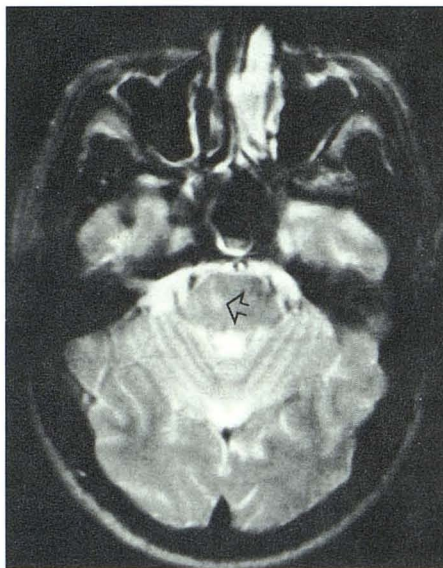
5

Fig. 6.—Axial 1.5-T SE 4300/80 image of normal 56-year-old shows decreased signal in lateral putamen (arrows).



6

Fig. 7.—Axial 1.5-T SE 4300/80 image of secondary parkinsonism—midbrain infarct (arrow).



7

Fig. 8.—Axial 1.5-T SE 4300/80 image of early progressive supranuclear palsy with increased signal in tectum (arrows).



8

ary parkinsonisms and heterogeneous system degenerations numerous changes were found.

Secondary parkinsonisms can occur after infection, be drug- or toxin-induced, or result from trauma or vascular causes. No drug-induced or postinfection cases were available for study. Excellent correlation occurred in acute parkinsonism suspected to be secondary to stroke. All four cases studied showed focal areas of increased signal in the midbrain at the level of the decussation of the brachium conjunctivum or upper pons compatible with infarcts (Fig. 7).

A third category of parkinsonism consists of heterogeneous system degenerations; that is, parkinsonism plus other clinical signs. Among this subgroup are several diseases: progressive

supranuclear palsy, olivo-ponto-cerebellar atrophy, Shy-Drager syndrome, and striatonigral degeneration.

Of this subgroup we studied six patients with progressive supranuclear palsy, all of whom had focal atrophy of the midbrain, particularly the tectum, with concurrent dilatation of the aqueduct, quadrigeminal plate cistern, and posterior portion of the third ventricle. In three of the cases increased signal was seen in the periaqueductal region and in one case the tectum. These cases were encountered early in their clinical course and showed less atrophy than the chronic cases (Figs. 8 and 9).

In four cases of olivo-ponto-cerebellar atrophy focal atrophy of the olives, pons, brachium pontis, medulla, and cerebellum

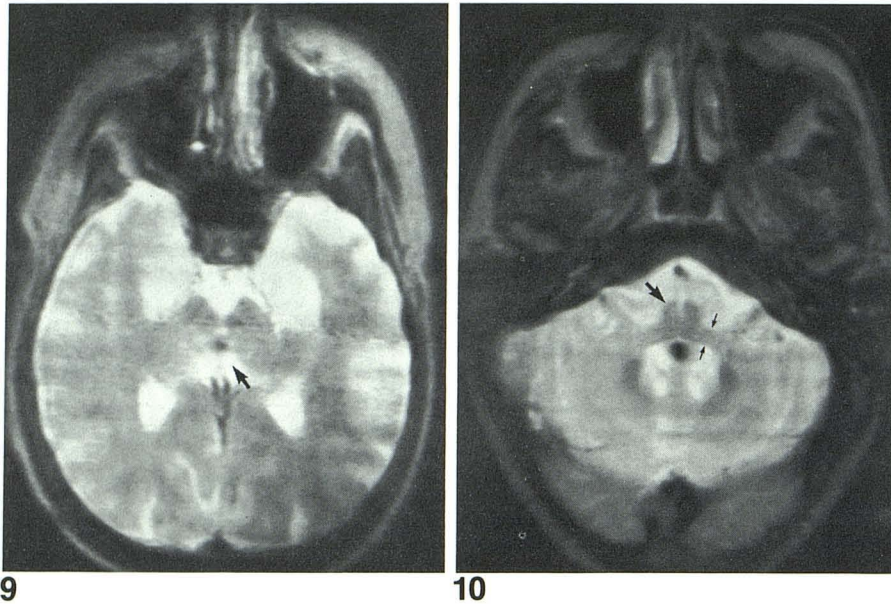


Fig. 9.—Axial 1.5-T SE 4300/80 image of chronic progressive supranuclear palsy with focal atrophy of tectum and enlargement of quadrigeminal plate cistern (arrow).

Fig. 10.—Axial 1.5-T SE 4300/80 image of olivo-ponto-cerebellar atrophy shows marked focal atrophy of pons (large arrow) and brachium pontis (small arrows).

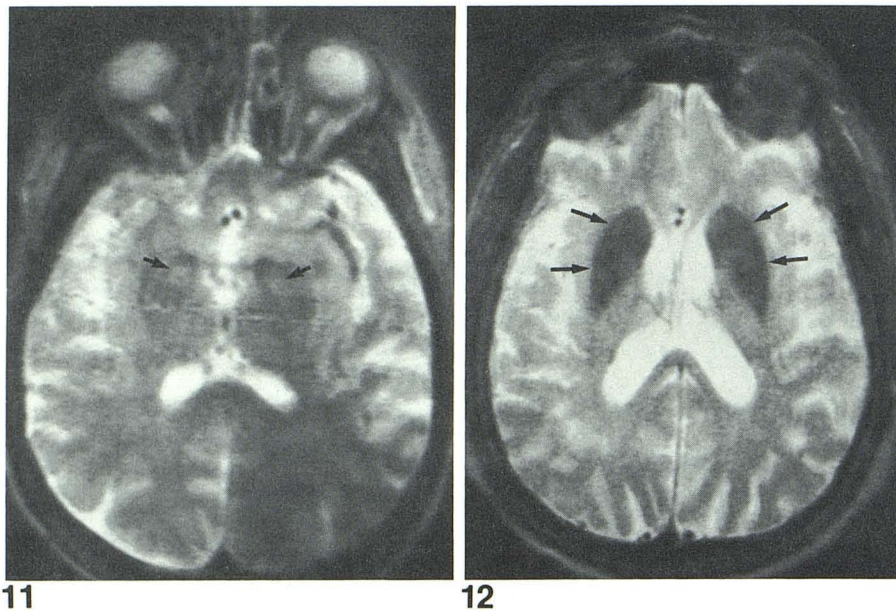


Fig. 11.—Axial 1.5-T SE 4300/80 image in Shy-Drager syndrome shows increased signal in globus pallidus (arrows).

Fig. 12.—Axial 1.5-T SE 4300/80 image of unclassified parkinsonism with homogeneous decreased signal throughout neostriatum (arrows).

was observed. No change in parenchymal signal was noted (Fig. 10).

In seven cases of Shy-Drager syndrome, atrophy similar to that of olivo-ponto-cerebellar atrophy was seen; and in four cases, increased signal was seen in the globus pallidus, which we attributed to advanced degeneration of the globus pallidus with gliosis (Fig. 11).

One case of striatonigral degeneration was observed and demonstrated atrophy of the caudate without other abnormality; motion limited fine detail in this case.

In addition, two cases of an unclassified disease with dramatic changes were observed. The cases demonstrated markedly decreased signal in the entire neostriatum, unlike

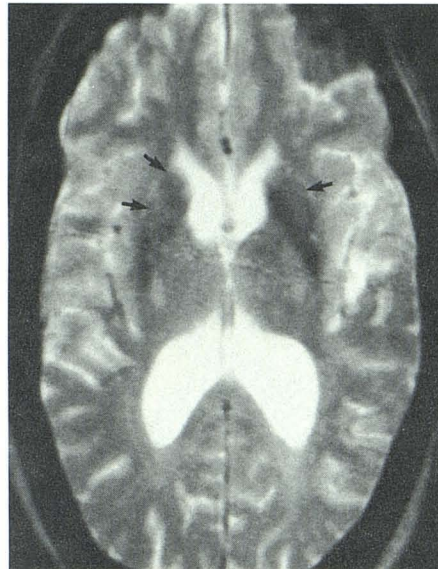
the normal controls, where signal void was spotty. Signal void in the putamen was pronounced and homogeneous with sharp margins (Fig. 12). Clinically, these cases manifested prominent rigidity, ataxia, and a poor response to treatment.

Six patients with myoclonus, two with focal and four with diffuse forms, were examined and showed no imaging abnormality.

Choreic Disorders and Hemiballismus

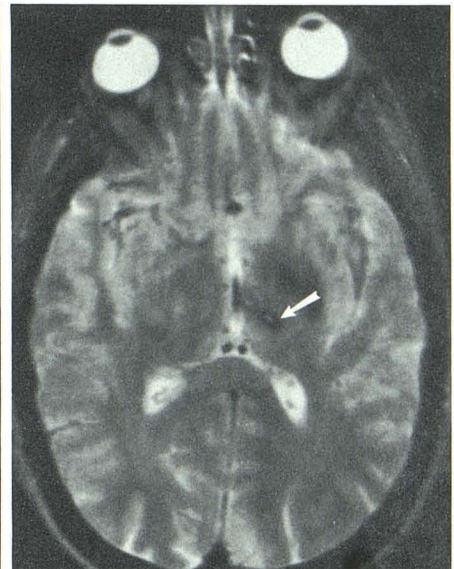
Eight patients with choreic disorders were imaged, four with Huntington's disease, three with chorea-acanthocytosis

Fig. 13.—Axial 1.5-T SE 4300/80 image in Huntington's chorea shows decreased signal and atrophy of neostriatum, predominantly caudate nucleus (arrows).



13

Fig. 14.—Axial 1.5-T SE 4300/80 image in hemiballismus secondary to hemorrhagic infarct in left subthalamic nucleus (arrow).



14

TABLE 4: MR Findings in Secondary Dystonias

Pathology: Signal Abnormality	No. of Patients (n = 41)
Leigh's disease and subacute necrotizing encephalopathy:	
Increased signal, putamen, midbrain, and cortex	5
Postinfarct dystonia:	
Increased signal, putamen	3
Decreased signal, putamen (hemorrhagic)	3
Postinfection dystonia:	
Increased signal and atrophy, putamen	2
Metabolic aciduria (glutaric):	
Increased signal, neostriatum (primarily putamen)	1
Glioma:	
Increased signal, basal ganglia	1
Wilson's disease:	
Decreased signal, neostriatum, at high field	1
Previous perinatal ischemic insult:	
Mild decreased signal, neostriatum	3
Hallervorden-Spatz disease:	
Increased and decreased signal, globus pallidus	4
Unknown metabolic disorder:	
Multiple areas decreased signal basal ganglia	1
Unclassified (for example, ?Leigh's disease, ?neuroaxonal dystrophy):	
Increased signal, neostriatum	9
Total	33

(CAC), and one with Sydenham's chorea. In this series, all patients with Huntington's disease and CAC showed decreased signal in the neostriatum, caudate, and putamen (Fig. 13). Generalized atrophy as well as focal atrophy of the neostriatum, predominantly of the caudate, with resulting enlargement of the frontal horns was seen in six of the seven cases. The patient without significant atrophy was in an early

stage of Huntington's disease with only mild choreic movements. No significant difference was noted between images of Huntington's disease and CAC. One CAC patient was imaged twice over a 6-month period. A modest decrease in the signal of the neostriatum accompanied a progressive worsening of his clinical symptoms. The single case of Sydenham's chorea imaged showed no abnormalities. The patient was improving at the time of examination and went on to full recovery.

Four patients with hemiballismus were studied. All cases were of acute onset and demonstrated signal changes in the contralateral subthalamic nucleus region. Three of the patients demonstrated increased signal compatible with infarct, and one patient demonstrated increased signal surrounded by decreased signal compatible with subacute hemorrhage (Fig. 14).

Dystonias

Sixty patients with various dystonic conditions were examined. Nineteen were classified as primary dystonias and 41 were classified as secondary dystonias. No specific anatomic changes were noted in the dystonia group as a whole. The primary dystonia group comprised eight generalized (dystonia musculorum deformans) and 11 focal (for example, spasmodic torticollis and Meige syndrome) dystonias. No signal abnormalities were seen in any patient with a primary dystonia.

Thirty-three (80%) of the 41 patients with secondary dystonia, sudden- or delayed-onset dystonia, demonstrated signal changes in the neostriatum or paleostriatum. Twenty-one of these showed increased signal in the caudate and putamen, eight showed decreased signal in the caudate and putamen, and four showed mixed increased and decreased signal in the globus pallidus. Focal atrophy was seen in three patients in the putamen associated with increased signal.

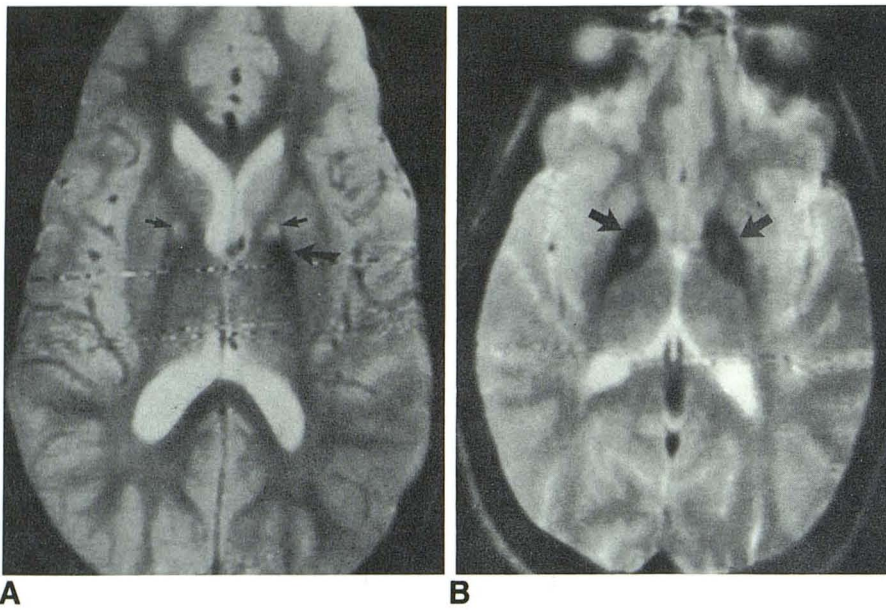


Fig. 15.—Axial 1.5-T SE 4300/80 images in Hallervorden-Spatz disease.

A, Increased (small arrows) and decreased (large arrow) signal in globus pallidus.

B, Another patient. More uniformly decreased signal in globus pallidus bilaterally with slight central increased signal in long-standing disease (arrows).

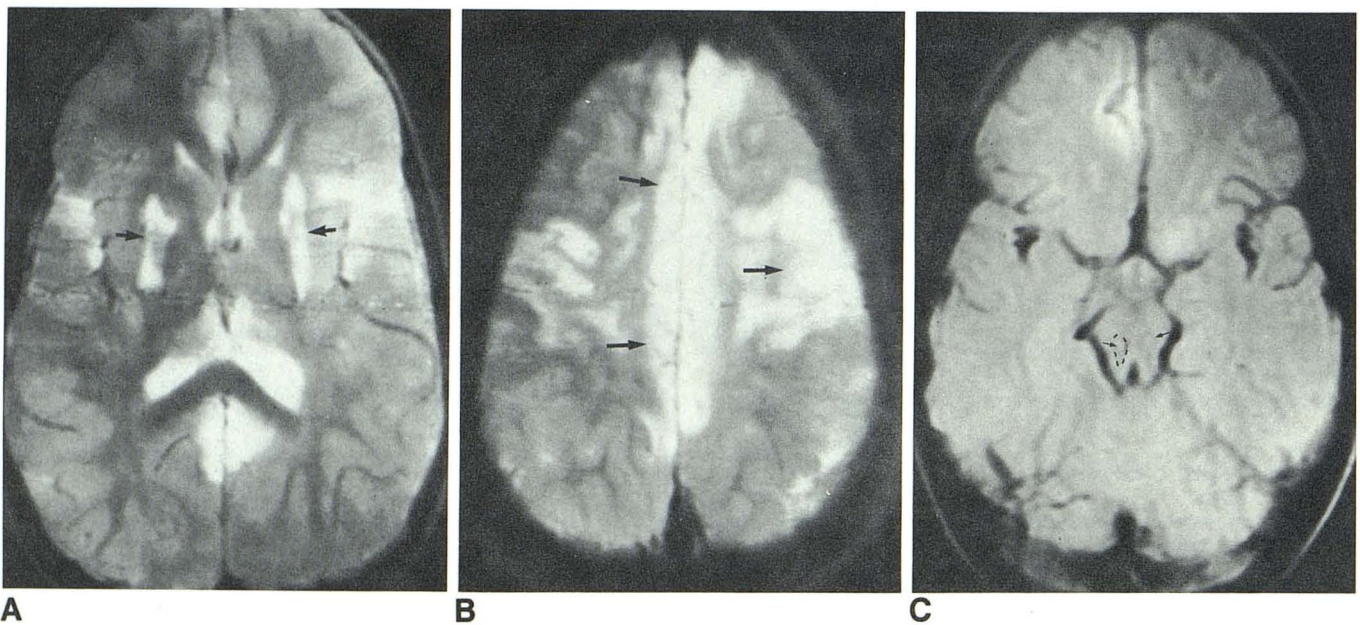


Fig. 16.—Axial 1.5-T MR images in Leigh's disease.

A, SE 4300/80. Increased signal in both putamen (arrows).
B, Additionally increased signal in cortical areas (arrows) in subacute necrotizing form.

C, SE 2000/80 image. "Butterfly" pattern of periaqueductal increased signal (arrows) is characteristic of Leigh's disease.

When assessed by clinical diagnosis, even more discernible patterns were found in secondary dystonia (Table 4). Four patients with strong clinical/familial evidence of Hallervorden-Spatz disease (HSD) demonstrated markedly decreased signal in the globus pallidus when compared with the normal signal loss in the red nucleus (Fig. 15). Small areas of increased signal were also seen within the areas of decreased signal. No focal atrophy was seen in these patients. Their CT scans demonstrated little or no calcification in the globus

pallidus. Several cases of clinically suspected neuroaxonal dystrophy, believed by some to be related to HSD (symptomatically similar but with an earlier age of onset), were grouped with cases of progressive unclassified dystonias; all showed increased signal in the putamen.

Four cases of confirmed Leigh's disease showed changes similar to those of the unclassified group of progressive dystonias with increased signal in the neostriatum, predominantly the putamen. In addition, in one patient with subacute

necrotizing encephalopathy, a cortical form of Leigh's disease, increased signal was observed in the cortex and mid-brain and was equivalent to the described diagnostic pathologic changes (Fig. 16).

One patient with glutaric aciduria was studied at 6 and 8 months of age. The first images were normal for age; the second showed increased signal in the neostriatum similar to that of the above cases (Fig. 17). Other cases demonstrating increased signal in the neostriatum included two cases of postinfection dystonia and three cases of infarct-induced dystonia (Figs. 18 and 19). These cases also demonstrated atrophy in associated structures. In one case of basal ganglionic glioma with dystonia increased signal was seen also.

Three patients with a history of perinatal ischemic insults with resulting dystonia showed mildly decreased signal in the neostriatum. Two cases with this tenuous diagnosis were normal. One case of Wilson's disease showed bilateral decreased signal in neostriatum (Fig. 20). Three cases of infarct-induced dystonia showed decreased signal unilaterally in the putamen compatible with posthemorrhagic deposition of hemosiderin. One presumed metabolically caused dystonia showed multiple areas of decreased signal throughout the basal ganglia in a heterogeneous pattern.

Nine patients fell into an unclassified group because of a lack of definitive pathologic or clinical/laboratory proof. These cases all had similar findings with increased signal observed in the neostriatum predominantly the putamen. No changes in the globus pallidus were seen in the suspected neuroaxonal dystrophy. Several cases that may be Leigh's disease were also left unclassified pending pathologic proof.

Of the eight cases of secondary dystonias with no signal abnormality, two were believed to have been caused by perinatal ischemic insults, one was a 69-year-old with marked generalized atrophy, one was associated with Behr's syndrome, one was later determined to be a hysterical dystonia,

two were believed to have resulted from drugs or toxins, and one occurred after head trauma.

Discussion

General

The clinical features of movement disorders often bear little resemblance to the gross pathologic changes. Biochemical abnormalities are the cause of many manifestations and are reflected only secondarily by structural changes such as atrophy or cell loss. The nature of movement disorders is also, like most neurodegenerative disorders, associated with a long clinical course that does not allow simple clinicopathologic correlation. The final autopsy findings also may not reflect the dynamic changes that can be captured by *in vivo* imaging methods. Because of these limitations, our analysis tried to group patient images first by the overt clinical dyskinesia and second by the clinical diagnosis. Limitations in the ability to verbally describe movement has always been a handicap and of necessity required a simplified group of definitions (Table 1). The rarity of many of the disorders also limits observation. Some of the diseases, therefore, are poorly defined. The simplified extrapyramidal system schema was then introduced to correlate anatomic regions of abnormality in relation to abnormal movement and to avoid memorizing the findings in a large number of rare diseases.

Iron/MR Correlation

To fully exploit the ability of MR imaging to map iron, more precise knowledge about its functions in the brain, its distribution at the cellular level, and the physical state in its many roles is required. Also, an explanation for the close but imperfect correlation with iron staining is necessary (Fig. 4).

Fig. 17.—Axial 1.5-T SE 4300/80 image in 8-month-old patient with glutaric aciduria. Increased signal in neostriatum, predominantly putamen (arrows).



17

Fig. 18.—Axial 1.5-T SE 4300/80 image in subacute postinfection dystonia shows atrophy and increased signal in putamen (arrows).



18

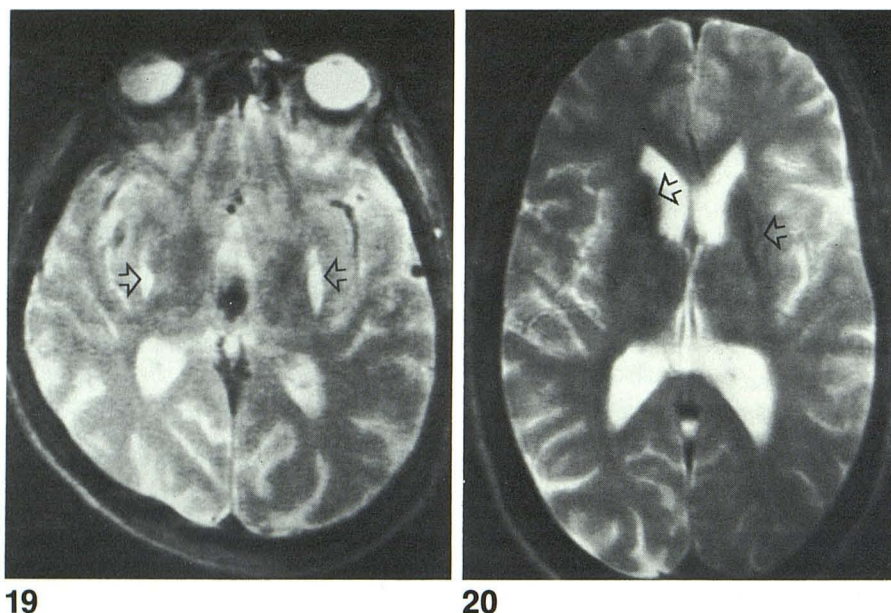


Fig. 19.—Axial 1.5-T SE 4300/80 image after anoxic infarct-induced dystonia shows increased signal in putamen bilaterally (arrows).

Fig. 20.—1.5-T SE 4300/80 image in Wilson's disease shows decreased signal and atrophy secondary to copper deposition in neostriatum (arrows).

Functionally, iron is required in oxidative metabolism at every step of the electron transport chain. This alone cannot, however, account for the very large variation of iron concentration in different parts of the brain, since there are no significant differences in metabolic rates of the cerebral cortex and basal ganglia as evaluated by positron emission tomography (PET) and other methods. Iron also participates in enzymatic synthesis of biogenic amines (dopamine, norepinephrine, and serotonin), and this may be relevant to regional metabolism. It should be noted, however, that high levels of iron are not always found in catecholaminergic (for example, nigra compacta, locus ceruleus) or serotonergic (for example, median raphe) systems [14–16]. The coincidence of iron and gamma-aminobutyric acid (GABA)-rich structures [17] is also imperfect (for example, the hypothalamus and superior colliculus) [18], while possible roles for iron in peptidergic systems are speculative [19].

If these known enzymatic requirements for iron are added to the amount stored as ferritin (estimated at one-third to one-half of the total), the sum still does not account for the high content of iron in specific regions of the brain. Therefore, it is possible that the regional concentrations of iron reflect neural system-specific functions that remain unknown.

Perls' Prussian blue reaction, long considered a highly sensitive method for the histochemical detection of ferric iron, colors specific regions consistently, but what proportion of the iron in the tissue is reactive (hemoglobin iron is not) and how much of it is solubilized in the process and subject to diffusion has not been determined. Also, cellular localization and changes with age and maturity are not always in accord [20–27]. With advancing age, encrustations of blood vessels in the globus pallidus, cerebellum, and hippocampus are seen and doubtless represent a special aspect of regional iron metabolism in tissue assay and imaging.

The biochemical versatility of iron is understandable in

terms of this metal's extraordinary range of oxidation states, from Fe(II) to Fe(VI), which explains its active presence along the entire chain of electron transfer reactions [28]. Only Fe(II) and Fe(III) are stable in aqueous solution, but with ligands, marked displacements of valence electrons from the d orbitals take place. Such spatial rearrangements have profound effects on stereochemical binding properties, and in this regard, it is interesting to speculate that the disparity between the neostriatal and pallidonigral imaging and iron staining is caused by iron in the two structures in predominantly different forms (and subserves different functions).

In a study of the relaxation of water in the presence of ferritin, Koenig et al. [1] showed that the relaxation behavior of ferritin changes with the amount of iron within its core. A core substantially loaded with iron has no effect on T1, but has a substantial shortening effect on T2. Ferritin molecules with partially loaded cores do not demonstrate these changes. Koenig et al. postulated that the pronounced T2* effect is the result of small ferrimagnetic domains of ferric or mixed valence oxides produced within the core. This suggests that at least some of the failure of correlation between Perls' Prussian blue reaction and the heavily T2-weighted images can be attributed to states in which ferric iron is isolated within ferritin.

Parkinsonism

Describing changes in the images of patients with parkinsonism finds clinical utility in the ability to differentiate primary parkinsonism (Parkinson's disease) from secondary parkinsonisms and hereditary system degenerations. Clinically, Parkinson's disease consists of a tetrad of findings: rigidity, bradykinesia, postural instability, and resting tremor. Secondary parkinsonisms and hereditary system degeneration may also manifest these symptoms initially. That these groups of diseases can be differentiated by imaging has been suggested

by CT studies [29], and imaging is improved with MR because of its increased sensitivity to pathology and ability to differentiate the iron-containing extrapyramidal nuclei.

This sensitivity is seen in Parkinson's disease as restoration of signal in the dorsal lateral substantia nigra, hypothesized to be caused by either depletion of iron by increased cellular metabolic activity or by local cell death resulting in expansion of the extracellular space, which overwhelms the T2* effect by increasing signal locally [30]. Supporting this, PET has documented increased metabolism in the basal ganglia, and drug therapy has been shown to increase metabolic activity in the region [31, 32]. The inconstant occurrence (75%) requires further assessment regarding the age of the patient, therapeutic regimen, angle of the imaging plane, and specific clinical manifestations. That 53% of normal patients over 50 also have this change may suggest a threshold effect is present.

In secondary parkinsonism the increased sensitivity to cell loss; demyelination; and edema from infarcts, trauma, infections, toxins, and multiple sclerosis allows differentiation. In the group of heterogeneous system degenerations increased sensitivity is reflected primarily by detection and assessment of atrophy patterns. Occasionally, signal changes also are helpful. In supranuclear palsy these signal changes preceded the clinical changes. In these early cases, we hypothesize that increased signal seen in the periaqueductal and tectal regions represents gliosis and that atrophy occurs as the condition progresses [33]. In Shy-Drager syndrome, differentiation from olivo-ponto-cerebellar atrophy can be made by increased signal changes in the globus pallidus. This was only present in half of our cases and underscores the pathologic similarity between these diseases [34, 35]. Unlike other descriptions, we found no excess in iron. This is not surprising, as a review of this disorder by Schwarz [36] found no pathologic increase in iron. We suspect that, because of their similarity, olivo-ponto-cerebellar atrophy and Shy-Drager syndrome are linked in the multifocal atrophies. Another similar condition, striatonigral degeneration, is noteworthy in that it also does not demonstrate increased iron pathologically [37].

The two cases with homogeneous signal loss in the neostriatum underscore the utility of MR imaging. While clinically these patients were characterized by changes similar to olivo-ponto-cerebellar atrophy (ataxia, bradykinesia, mild tremor, and rigidity), they were clinically differentiated by poor responses to treatment. Other investigators have attributed this pattern to Shy-Drager syndrome, but our patients had no autonomic findings, considered a prerequisite of the syndrome [12]. Taking this into account, we believe that this change is either nonspecific, that it represents a separate disease, or that Shy-Drager syndrome may not always manifest with autonomic dysfunction.

Although the myoclonus cases imaged demonstrated no changes, it is believed that this group is worth imaging. An acquired form (hypoxic, infectious, and degenerative), as well as a familial form, exists. Pathologic changes described in the familial form may be too subtle for imaging, but changes in the acquired form may be recognizable [38].

Choreic Disorders and Hemiballismus

The prototypic choreic disorder is Huntington's disease, which is caused by a genetic abnormality in the short arm of the fourth chromosome resulting in loss of a specific set of cholinergic and GABA-nergic neurons and metabolic activity in the neostriatum [8, 30]. The recent ability to detect the chromosomal abnormality precludes much of the potential utility of the MR changes, even the suggestive loss of signal before atrophic changes. In the similar pathologic entity of chorea-acanthocytosis, distinguished by acanthocytes in the blood, MR changes are identical to those in Huntington's disease and suggest a residual utility and commonality of findings and location for choreic disorders. The decreased neostriatal signal corresponds to the increased iron described by Hallervorden [39] and Terplan [40]. In our one case of Sydenham's chorea with no MR abnormalities, progressive improvement, and full recovery, it is interesting to speculate if imaging findings are predictive.

Hemiballismus is a rare disorder caused by stroke, hemorrhage, or tumors damaging the contralateral subthalamic nucleus or, less often, the striatum or thalamic nuclei. Since the pathology is so well described and specific, imaging changes should be present and diagnostic in all cases. Imaging may be of value in subacute and borderline choreic cases and for differentiating the rare neoplastic etiologies.

Dystonia

Like the other groups, this group showed greatest correlation when subdivided by clinical diagnoses. That this assessment can then differentiate primary and secondary dystonia is not surprising. Primary dystonias (for example, dystonia musculorum deformans) have no known pathology, and secondary dystonias, which are associated with metabolic diseases, have several known pathologic changes. In this context, primary dystonias are defined as action dystonias, insidious in onset and slowly progressive with late posturing. Secondary dystonias are defined as sudden- or delayed-onset dystonias at rest with sustained postures and a more rapidly progressive course [41].

In trying to classify the secondary dystonias, it was found that an association with individual disease was stronger than any classification, such as hereditary and acquired forms. Wilson's disease is a good example, demonstrating a decreased signal in the putamen from the T2* effect of the copper, deposited due to a derangement in metabolism. Leigh's disease, a defect in pyruvate metabolism with a resulting elevation in lactate levels, demonstrates the opposite, increased signal in the putamen. At low field strengths, increased signal has been reported in Wilson's disease [42, 43] and probably reflects the inability to detect T2* effects at low field or variation in the amount of copper deposition.

When considering separately the diagnosis of HSD, a high field strength is advantageous in detecting the T2* of the increased iron in the globus pallidus. Pathologically, the globus pallidus also shows demyelination, neuronal loss, gliosis, and focal axonal swelling [44], which on T2-weighted images are reflected by increased signal. It is suspected that these

changes account for the heterogeneous signal pattern on our images. That our suspected cases of neuroaxonal dystrophy have no decreased signal on T2-weighted images in the globus pallidus suggests that HSD and neuroaxonal dystrophy should be considered as separate diseases despite the arguments of a shared metabolic defect [45–47].

In considering Leigh's disease, in addition to the increased signal in the putamen denoting its dystonic nature, signal changes in the midbrain and cortex suggest a feature differentiating it from the other dystonias. Pathologically, the periaqueductal signal changes correlate with gliosis and vacuolation [48]. In the cortical form a spongiform degeneration has been described. All the pathologic changes share the common MR finding of increased signal.

The one case of glutaric aciduria is important because it represents a large group of amino acid metabolic defects that are potentially treatable. The pathologic lesions manifest by these disorders are probably secondary to local acidosis, hypoglycemia, or hyperammonemia. The resulting cell loss and gliosis is detected by increased signal on T2 images. Also described histologically is a failure of myelination that we have seen in another case of aminoaciduria without dystonia or lesions in the putamen.

In the two cases of postinfection secondary dystonia increased signal and mild atrophy were seen in the putamen. No additional distinguishing features were found to separate this diagnosis from the others. An immunologic etiology is suspected, and little pathologic data are available.

In the five patients with the clinical diagnosis of perinatal ischemia a strong clinical interest exists because, unlike most of the other dystonias, these disorders are relatively static. The lack of a well-defined subset of asphyxia neonatorum producing pathologic changes consistent with our findings and the sparse historical data available make any conclusions highly speculative. However, experimental work by Windle [49] on rhesus monkeys suggests that perinatal ischemic insults as well as other factors may result in hemorrhage or other abnormalities such as mineral deposition that could result in decreased signal.

In the eight cases of infarct-induced dystonia a consistent pattern of putamenal lesions was found. Unique to MR was the ability to differentiate whether these were hemorrhagic or not, even when the ictus was in the distant past. The post-hemorrhagic deposition of hemosiderin demonstrates a decrease in signal on the T2 image secondary to the T2* effect. The vascular distribution in the neostriatum is such that it is rarely affected by embolic events in isolation, and so generalized ischemia (such as carbon monoxide poisoning) and localized ischemia, hemorrhage, or thrombosis (by atherosclerosis or dystrophic changes of the lenticulostriate arteries associated with hypertension or occlusive arterial diseases) can be considered as causes of these secondary dystonias.

The unclassified group of dystonias may represent several diagnoses, including Leigh's disease, neuroaxonal dystrophy, or other metabolic abnormalities, but gives support to the idea that increased signal in the putamen is closely associated with dystonic movements. Further histologic investigation will determine if separate disease entities are present.

In the eight cases of secondary dystonias in which no signal abnormality was seen, it can only be assumed, without pathologic data, that these represent metabolic abnormalities not identified or structural abnormalities beyond the resolution of MR. In the case of hysterical dystonia, the normal examination strongly weighted the approach to treatment.

Conclusions

The ability to image the nuclei of the extrapyramidal motor system allows us to correlate, in life, many structural defects with functional deficits. Two of the largest gaps in this correlation at the present time are (1) the lack of correlation between chemically demonstrated iron distribution and metabolism and (2) imperfect correlation between the signal void on T2-weighted images and sections of the brain treated with Perls' stain.

In general, the MR brain findings in patients with movement disorders consist of complex patterns of focal atrophy, regions of pronounced signal void on T2-weighted images, and regions of increased signal in the various extrapyramidal nuclei. More specifically, in parkinsonisms we see a restoration of signal in the substantia nigra as well as less specific forms of atrophy. In choreas we see decreased signal in and atrophy of the caudate nucleus and to a lesser extent the putamen. In hemiballismus we see an increased signal in the subthalamic nucleus. In dystonias, we see no specific abnormalities in primary dystonia but often see abnormal signal in the neostriatum, especially the putamen in secondary dystonias (Tables 3–5).

While strict anatomic localization of pathology in these conditions is still in its early stages, we believe that this classification, while simplified [50, 51], has significant utility in clinical diagnosis.

ACKNOWLEDGMENTS

We thank Susan Bressman, Mitchel Brin, Lucien Cote, and Darryl DeVivo for sharing their patients and clinical diagnoses; Howard Radzyner for photography; and Charles Deschamps for imaging.

REFERENCES

1. Koenig SH, Brown RD, Peters TJ, Ward RJ. Relaxometry of ferritin solutions and the influence of the Fe(III) core ions. *Magnetic Resonance Med* 1986;3:755–767
2. Rutledge JN, Hilal SK. MRI imaging of movement disorders (abstr). *Radiology* 1985;157:290
3. Harrison WW, Netsky MG, Brown MD. Trace elements in human brain: copper, zinc, iron, and magnesium. *Clin Chim Acta* 1968;21:55–60
4. Hock A, Demmel U, Schicha K. Trace element concentration in human brain. *Brain* 1975;98:49–64
5. Ule G, Volkl A, Berlet H. Trace elements in human brain. *Neurology* 1974;206(2):117–128
6. Hallgren B, Sourander P. The effect of age on the non-haemin iron in the human brain. *J Neurochem* 1958;3:41–51
7. Seab JA. Anatomy and pathology of extrapyramidal diseases. *Brain Res Bull* 1983;11:135–141
8. Cote L, Crutcher M. Motor functions of the basal ganglia and diseases of transmitter metabolism. In: Kandel ER, Schwartz JH, eds. *Principles of neural science*, 2d ed. New York: Elsevier, 1985:523–534

9. Yung CY. Clinical features of movement disorders. *Brain Res Bull* **1983**;11:167-171
10. Gans A. Iron in the brain. *Brain* **1923**;46:128-136
11. Drayer B, Burger P, Darwin R, Riederer S, Herfkens R, Johnson GA. Magnetic resonance imaging of brain iron. *AJNR* **1986**;7:373-380
12. Drayer BP, Olanow W, Burger P, Johnson GA, Herfkens R, Riederer S. Parkinson plus syndrome: diagnosis using high field MR imaging of brain iron. *Radiology* **1986**;159:493-498
13. Pastakia B, Polinsky R, DiChiro G, Simmons JT, Brown R, Wener L. Multiple system atrophy (Shy-Drager syndrome): MR imaging. *Radiology* **1986**;159:499-502
14. Mackler B, Person R, Miller LR, Indamar AP, Finch CA. Iron deficiency in the rat: biochemical studies of brain metabolism. *Pediatr Res* **1978**;12:217-220
15. Sourkes TL. Transition elements and the nervous system. In: Pollitt E, Leibel RL, eds. *Iron deficiency: brain biochemistry and behavior*. New York: Raven, **1982**:1-29
16. Youdim MBH, Green AR, Bloomfield MR, Mitchell BD, Heal DJ, Grahame-Smith DG. The effects of iron deficiency on brain biogenic monamine biochemistry and function in rats. *Neuropharmacology* **1980**;19:259-267
17. Francois C, Nguyen-Legros J, Percheron G. Topographical and cytological localization of iron in rat and monkey brains. *Brain Res* **1981**;215:317-322
18. Roberts E, Chase TN, Tower DB, eds. *GABA and central nervous system function*. New York: Raven, **1976**:169-186
19. Sullivan S, Akil J, Blacker D, Barchas JD. Enkephalinase: selective inhibitors and partial characterization. *Peptides (Fayetteville)* **1950**;1:31-35
20. Hill JM. Brain iron: sex difference and changes during the estrous cycle and pregnancy. In: Saltman P, Hegenauer J, eds. *The biochemistry and physiology of iron*. New York: Elsevier Biomedical, **1982**:599-601
21. Dallman PR, Siimes MA, Manies EC. Brain iron: persistent deficiency following short-term iron deprivation in the young rat. *Br J Haematol* **1975**;31:209-215
22. Dallman PR, Spirito RA. Brain iron in the rat: a possible basis for irreversible depletion of brain non-heme iron following a brief period of iron deficiency. In: Brown EB, Aissen P, Fielding J, Crichton RR, eds. *Proteins of iron metabolism*. New York: Grune & Stratton, **1977**:381-386
23. Hill JM, Switzer RC. The regional distribution and cellular localization of iron in the rat brain. *Neuroscience* **1984**;11:596-603
24. Barden H. The histochemical distribution and localization of copper, iron, neuromelanin and lysosomal enzyme activity in the brain of aging rhesus monkey and the dog. *J Neuropathol Exp Neurol* **1971**;30:650-667
25. Kishi R, Ikeda T, Miyake H, et al. Regional distribution of lead, zinc, iron, and copper in suckling and adult rat brains. *Brain Res* **1982**;215:180-182
26. Spatz H. Eisennachweis im Gehirn, besonders in Zentren de extrapyramidalen Systems. *Eur Arch Psychiatry Neurol Sci* **1922**;77:261
27. Martin TL, Switzer RC, Joshi J, et al. Ferritin localization in rat brain by immunocytochemistry. *Soc Neurosci Abstr* **1985**;11:502
28. Spiro TG. Chemistry and biochemistry of iron. In: Brown EB, ed. *Proteins of iron metabolism*. New York: Grune and Stratton **1977**:xxiii-xxxii
29. Ambrosetto P, Michelucci R, Forti A, et al. CT findings in PSP. *J Comput Assist Tomogr* **1984**;8(3):406-409
30. Schoene WC. Degenerative diseases of the central nervous system. In: Davis RL, Robertson DM ed. *Textbook of neuropathology*. Baltimore: Williams & Wilkins, **1985**:788-823
31. Martin WR. Positron emission tomography in movement disorders. *Can J Neurol Sci* **1985**;12:6-10
32. Weiner W, Nausieda P, Klawans H. Effect of chlorpromazine on CNS concentration of manganese, iron and copper. *Life Sci* **1977**;20:1181-1186
33. Behrman S, Carrol J, Janata I, et al. Progressive supranuclear palsy: clinico-pathological study of 4 cases. *Brain* **1969**;92:663-678
34. Shy GM, Drager GA. A neurological syndrome associated with orthostatic hypotension. *Arch Neurol* **1959**;42:511-527
35. Petitto CK, Black IB. Ultrastructure and biochemistry of sympathetic ganglia in idiopathic orthostatic hypotension. *Ann Neurol* **1978**;4:417-433
36. Schwarz GA. Dysautonomic syndromes in adults. In: Vinken PY, Bruyn GW, eds. *Handbook of clinical neurology*, vol 22. Part 2. *System disorders and atrophies*. New York: Elsevier, **1975**:243-280
37. Adams RD, Bogaert LV, Ecken HV. Striato-nigral degeneration. *J Neuropathol Exp Neurol* **1964**;23:584-608
38. Hoehn MM, Cherington M. Spinal myoclonus. *Neurology* **1977**;27:942-946
39. Hallervorden J. *Handbuch der speziellen pathologischen Anatomie und Histologie*. Berlin: Springer-Verlag, **1957**:793
40. Terplan K. Zur pathologischen anatomie der chronischen progressiven chorea. *Virchows Arch [Cell Pathol]* **1924**;252:146-176
41. Fahn S. The varied clinical expressions of dystonia. *Neurol Clin* **1984**;2(3):541-553
42. Lukes SA, Aminoff MJ, Crooks L, et al. Nuclear magnetic resonance imaging in movement disorders. *Ann Neurol* **1983**;13(6):690-691
43. Aisen AM, Martel W, Gabrielsen TO, et al. Wilson's disease of the brain: MR imaging. *Radiology* **1985**;157:137-141
44. Dooling E, Schoene W, Richardson E. Hallervorden-Spatz syndrome. *Arch Neurol* **1974**;30:70-83
45. Cowen D. Infantile neuroaxonal dystrophy. *J Neuropathol Exp Neurol* **1963**;22(2):175-236
46. Vakili S, Drew AL, Von Schuching S, et al. Hallervorden-Spatz syndrome. *Arch Neurol* **1977**;34:729-738
47. Littrup PJ, Gebarski SS. MR imaging of Hallervorden-Spatz disease. *J Comput Assist Tomogr* **1985**;9(3):491-493
48. Egger J, Pincott JR, Wilson J, et al. Cortical subacute necrotizing encephalomyelopathy. *Neuropediatrics* **1984**;15:150-158
49. Windle WF. Brain damage at birth. Functional and structural modification with time. *JAMA* **1968**;209(9):1967-1972
50. Young AB, Penney JB. Neurochemical anatomy of movement disorders. *Neurol Clin* **1984**;2(3):417-433
51. Marsden CD. The pathophysiology of movement disorders. *Neurol Clin* **1984**;2(3):435-459